Al-Khwarizmi Engineering Journal
ISSN (printed): 1818 – 1171, ISSN (online): 2312 – 0789
Vol. 22, No. 3, September, (2026), pp. 111- 123

Al-Khwarizmi Engineering Journal

Modelling of a 4×4 Multivariable Distillation Column Using Pulse Function-Based System Identification

Layth S. Mahmood[1*], Khalid M. Mousa Al-zobai[2]
[1]*Midland Refineries Company, Ministry of Oil, Baghdad, Iraq*
[2]*Department of Chemical Engineering, College of Engineering, Al Nahrain University, Baghdad, Iraq*
*Corresponding Author's E-mail: layth.phche23@ced.nahrainuniv.edu.iq

(Received 14 November 2025; Revised 29 January 2026; Accepted 16 February 2026; Published 1 September 2026)
https://doi.org/10.22153/kej.2026.02.004

Abstract

Distillation columns are considered the most essential units in chemical and petrochemical industries, particularly in oil refineries. This study aims to create and evaluate the empirical model for a multicomponent distillation column. An experimental model was constructed to represent the nonlinear behaviour of the column. The column is treated as a multi-input multi-output dynamic system. The industrial distillation columns used in this study has a diameter of 2.2 m and a height of 16.6 m. It is equipped with 20 valve trays. The process currently operates at Al-Doura Refinery as a part of the Midland Refinery Company in eastern Baghdad, Iraq. To find the model that describes the system, four manipulated variables (reflux flow rate, reboiler heat duty, the light component fraction in the feed and feed flow rate) and four controlled output variables (the light component fraction in the top product, the light component fraction in the bottom, the flow rate of the top product and the flow rate of the bottom product) were selected. The experiments were conducted by applying a pulse for 300 s to each of the manipulated variables while keeping the remaining variables constant. A 4×4 matrix consisting of 16 transfer functions (most of them are second order) was obtained. Each equation represents the relationship between the manipulated and controlled variables. These equations form the base for advanced control strategies such as fuzzy logic control, model predictive control or and other modern control approaches.

Keywords: *Pulse function; modelling of distillation column; system identification; MIMO systems*

1. Introduction

Oil refineries are among the largest production facilities, which comprise numerous complex industrial units. These units are used to produce and refine various types of fuel and other products that form the foundation of many related industries [1] and [2]. The distillation column is among the most crucial components used in this industry. It relies on the difference in boiling points of petroleum compounds. Based on this physical property, crude oil is separated into various petroleum fractions, each with its own scientific and practical importance and uses [3], [4]. Distillation is regarded as a complex and difficult process because of its nonlinear behaviour, high interactions, overlaps among control loops and long delay time. It is more difficult than individual input–output systems (SISO) [5], [6]. Recently, interest in developing control systems has considerably increased, particularly in the petroleum industry, with a focus on controlling distillation columns. Digital computers, advanced control strategies, artificial intelligence algorithms, neural networks and predictive control have been used to improve control in this field [7], [8]. To design these control systems, a good dynamic model is needed, and such models can be obtained from either first principles or empirical data. The control of distillation columns is investigated using various techniques.

Researchers study process performance, disturbance effects, disturbance rejection, control loop interactions and decoupling [9], [10]. Understanding the dynamic behaviour is necessary to complete this assignment. Understanding the underlying thermodynamic and transport processes, confirming theoretical models, improving process conditions and connecting process inputs and outputs through empirical mathematical models all depend on experimental research. Based on this understanding, several models have been created to depict the unstable condition of distillation columns. Despite their widespread usage, computational simulations need to be verified using experimental data to guarantee correctness and dependability [11], [12]. Distillation column modelling is generally classified into three main categories: fundamental modelling, empirical modelling and hybrid modelling. Fundamental modelling is based on first-principle mass and energy balances. Empirical modelling relies on experimental data and input–output relationships. Hybrid modelling combines first-principle knowledge with data-driven techniques. Using the input and output data from the operation of the column, the empirical modelling constructs the relationship between the input and output. This method minimises processing and does not require understanding the internal dynamics of the column. However, real columns should be used for trials to apply this strategy. This method utilises the advantages of the previous two, but to do so, a well-structured model is needed, and we must decide which parts of the model to utilise empirical data and which to apply basic approaches to [13]–[15]. Marshall and Pigford introduced the first mathematical model for distillation columns in 1947, but it faced challenges in solving differential equations for simple columns. Subsequent models by Tetlo, Peiser and Grover, Morris and Svrcek and Wagner and Holland have also addressed energy and material balances simultaneously. However, a comprehensive understanding of the mass transfer characteristics of the components remains essential for effective modelling [12], [16]. Skogestad's simplifications of models, particularly in energy balance, vapour dynamics and liquid flow dynamics, are mentioned as a response to the challenges posed by complex differential equations [17]. A multivariable predictive model was studied using only two variables. The results showed that this strategy is better than a conventional method [18]. A mathematical model for a distillation column of a binary system (benzene and toluene) utilised in multivariable control systems was constructed by Wahid and Adi [19]. Methanol and water were separated using a laboratory distillation column, which was described. The column was modelled in a state space model [20]. This modelling approach facilitates a deep understanding of the inherent dynamic complexity of distillation columns.

It also provides a fundamental basis for the development of advanced control strategies, such as fuzzy logic control (FLC), model predictive control (MPC) and other modern approaches, which aim to enhance process stability and improve operational efficiency [21]. However, most of these works consider binary or laboratory columns, while our work focuses on a multicomponent industrial column with 4×4 multi-input multi-output (MIMO) behaviour. This work aims to develop a 4×4 empirical model of an industrial naphtha distillation column using pulse tests and system identification.

2. Theory and Mathematical Model

Sets of ordinary differential equations based on mass and energy balances around each distillation column tray, as well as the reboiler and condenser units, were used in model construction. It also contains a dynamic function for the reflux drum and reboiler unit, as well as a set of algebraic equations and correlations for predicting mass transfer rate and physical characteristics. Although most distillation processes involve several components, some of these columns can sometimes be approximated to binary or quasi-binary mixes to simplify the process. Studying their simplified situation will help us understand the fundamental structure of these equations. The following assumptions are considered [4], [22]:

- Feed is at the boiling point (saturated liquid), which means no sensible heat.
- Vapour holdup in each tray is ignored (given that the density of vapour is much less than the density of liquid, ignoring vapour holdup reduces the number of differential equations and simplifies the dynamic model).
- No chemical reaction takes place inside the distillation column (physical process).
- The column is perfectly insulated.
- Liquid and vapour are in equilibrium on each tray to eliminate mass transfer kinetics and simplify equilibrium calculations.
- Constant tray efficiency along the column is considered to avoid stage-by-stage efficiency variation.
- Liquid holdup varies from tray to tray.

- Constant pressure (totally condensate) is considered to remove pressure drop effects and simplify phase equilibrium.
- Reboiler and condenser dynamics are ignored with fast condenser level control.
- The relative volatility remains constant throughout the column to allow linear Vapour liquid equilibrium (VLE) and simplify composition calculations. It is represented by the following equation:

$$\boldsymbol{y_{n,i}} = \frac{\boldsymbol{\alpha x_{n,i}}}{\boldsymbol{1+(\alpha-1)x_{n,i}}} \quad \ldots(1)$$

Based on these assumptions, the distillation column dynamics may be expressed by the subsequent mass and heat balance equations:

$$Mass\ flow\ rate\ in - Mass\ flow\ rate\ out = Mass\ accumulation \quad \ldots(2)$$

$$Heat\ transfer\ in - Heat\ transfer\ out = Heat\ accumulation \quad \ldots(3)$$

Overhead reflex drum
Total mass balance

$$\frac{dM_d}{dt} = V_1 - (R + D) \quad \ldots(4)$$

Component mass balance

$$\frac{dM_d x_{d,i}}{dt} = V_1 y_{1,i} - (R + D)x_{d,i} \quad \ldots(5)$$

Total heat balance

$$C_d \frac{dM_d T_d}{dt} = H_1^V V_1 - H_d^L (R + D) - Q_c \quad \ldots(6)$$

For any tray (n) except feed tray,
Total mass balance

$$\frac{dM_n}{dt} = L_{n-1} + V_{n+1} - V_n - L_n \quad \ldots(7)$$

Component mass balance

$$\frac{dM_n x_{n,i}}{dt} = L_{n-1}x_{n-1,i} + V_{n+1}y_{n+1,i} - V_n y_{n,i} - L_n x_{n,i} \quad \ldots(8)$$

Total heat balance

$$C_n \frac{dM_n T_n}{dt} = H_{n-1}^L L_{n-1} + H_{n+1}^V V_{n+1} - H_n^V V_n - H_n^L L_n \quad \ldots(9)$$

where $L_0 = R$, $x_{0,i} = x_{d,i}$, $V_{N+1} = V_b$, $y_{N+1,i} = y_{b,i}$, $H_0^L = H_R$, $H_{N+1}^V = H_b^V$.

For feed tray (nf),
Total mass balance

$$\frac{dM_{nf}}{dt} = L_{nf-1} + V_{nf+1} + F - V_{nf} - L_{nf} \quad \ldots(10)$$

Component mass balance

$$\frac{dM_{nf}X_{nf,i}}{dt} = Fx_{f,i} + L_{nf-1}x_{nf-1,i} + V_{nf+1}y_{nf+1,i} - V_{nf}y_{nf,i} - L_{nf}x_{nf,i} \quad \ldots(11)$$

Total heat balance

$$C_{nf} \frac{dM_{nf}T_{nf}}{dt} = H_{nf-1}^L L_{nf-1} + H_{nf+1}^V V_{nf+1} + H_f F - H_{nf}^V V_{nf} - H_{nf}^L L_{nf} \quad \ldots(12)$$

For the bottom of column,
Total mass balance

$$\frac{dM_b}{dt} = L_N - V_b - B \quad \ldots(13)$$

Component mass balance

$$\frac{dM_b X_{b,i}}{dt} = L_N x_{N,i} - V_b y_{b,i} - Bx_{b,i} \quad \ldots(14)$$

Total heat balance

$$C_B \frac{dM_b T_b}{dt} = H_N^L L_N + Q_R - H_b^V V_b - H_b^L B \quad \ldots(15)$$

Vapour liquid equilibrium

$$y_{n,i}^* = K_{n,i}x_{n,i} \quad \ldots(16)$$

where $K_{n,I}$ is the equilibrium factor

$$K_{n,i} = \frac{\gamma_{n,i}p_{n,i}^*}{\varphi_n p_n^T} \quad \ldots(17)$$

3. Experimental Work

The distillation column used in this study operates according to an LV configuration, which is a special type of control structure. It is commonly used in binary distillation processes. In this configuration, the manipulated variables are the liquid flow rate (L) and the vapour flow rate (V). Both serve as control inputs, along with the feed rate (F) and its concentration (X_f). This structure ensures efficient and stable separation performance under dynamic operating conditions [23].

In Fig. 1, a basic continuous distillation column for two products is displayed. The distillation column utilised in this study is 2.2 m in diameter and 16.6 m in height. It holds 20 trays of the valve tray type. The process currently operates at Al-Doura Refinery as a part of the Midland Refinery Company in eastern Baghdad, Iraq. The reboiler at the bottom of the column supplies the energy required for the operation. The air cooler condenser fully condenses the abovementioned vapours. At the feed tray (13), the feedstock, which is a multicomponent combination, enters the column as a saturated liquid (q = 1). The column is separated into a stripping section and a rectifying section by this tray. The main components of feedstock are light naphtha (pentane, hexane and their isomers) and heavy naphtha (heptane, octane, nonane and decane with their isomers), and they are treated as a pseudo-binary combination.

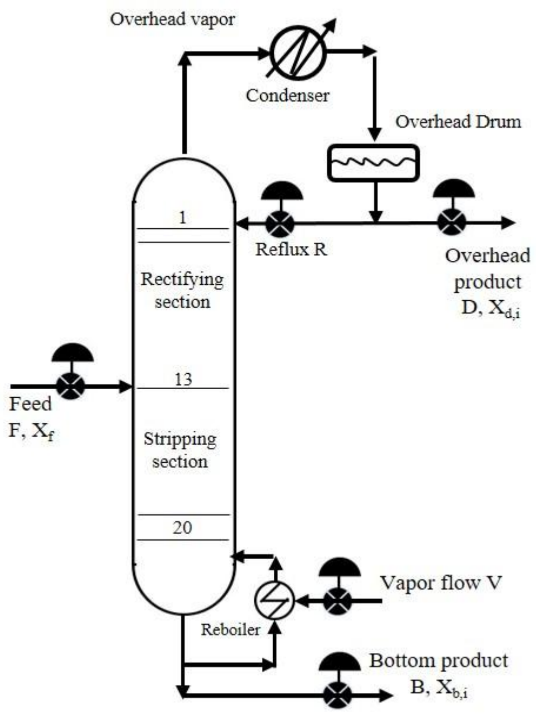

Fig. 1. Simple continuous distillation column controlled with LV configuration

Table 1 lists the operating parameters and steady-state data of the naphtha separation distillation column (used as a starting point for each experiment). To test the dynamics around this steady state, process reaction curve (PRC) experiments were performed on each manipulated variable. This process illustrates how changes in the single manipulated variable (MV) (inputs) affect the control variables (CVs) (outputs). The temperatures at the top and bottom of the distillation column were utilised as indicators of the proportion of light compounds, which are denoted as (X_d) and (X_b), respectively. In this investigation, four manipulated variables that had an impact on the four control variables were chosen, as shown in Table 2. Consequently, 16 PRCs will be produced if the four MVs are changed separately.

The temperature and the proportion of light components at the top and bottom of the column were found to be related in the shape of a curve. The proportion of each component in the mixture was determined by analysing the top and bottom products using the gas chromatography technique at various temperatures.

Table 1,
Steady-state data for the naphtha separation distillation column.

Variable	Feed	Top Product	Bottom Product
Flow rate (kg/h)	54,000	19,500	34,500
Light compound fraction (wt%)	41.05	87.71	14.5
Heavy compound fraction (wt%)	58.11	11.56	84.6
Other compounds	0.84	0.73	0.9
Temperature (°C)	102	100	130

Table 2,
Control variables (CV) and manipulated variables (MV).

Control variables (CV)	Manipulated variables (MV)
Light compound fraction in the top product (X_d) (wt%)	Reflux flow rate (R) (kg/h)
Light compound fraction in the bottom product (X_b) (wt%)	Reboiler heat duty
Top product (D) (kg/h)	Light compound fraction in the feed (X_f) (wt%)
Bottom product (B) (kg/h)	Feed flow rate (kg/h)

Applying a short-duration input signal to the system and monitoring its output lead to a matrix that represents the modelling of the processes. The pulse signal is useful for stimulating the dynamics of the system given that it has a wide variety of frequency components despite having a longer time span than an impulse. The output results, which are known as the pulse response, show how the system responds to abrupt input changes.

All experimental works were conducted on the industrial distillation column by applying a pulse for 300 s in one of the manipulated variables while keeping the rest of the variables constant. An appropriate pulse size was selected for each manipulated variable to ensure that it was sufficiently large to produce a measurable response in control variable. The pulse was carefully limited to prevent excessive oscillations that could drive the control loops beyond their operational limits. If the pulse is too small, then the resulting changes in the controlled variable may be unclear. Such small responses could be confused with the natural oscillations of the system or with noise from the process and control devices. The response of the controlled variables with time was recorded.

3.1 Pulse in Reflux Flow Rate

A pulse was applied to the upper reflux flow for 300 s, after which the flow was returned to its original value. This condition resulted in a decrease in the top-column temperature and, consequently, a reduction in the concentration of heavy components (C7+) in the distillate. This reduction led to an increase in the fraction of light components. After a certain time delay, the bottom temperature of the column also decreased, which caused an increase in the concentration and flow rate of light components in the bottom product, as shown in Figs. 2 and 3. These observations are consistent with those in previous studies [7], [22], [24]. Consequently, the distillate flow rate decreased (Fig. 4), while the bottom product flow rate increased (Fig. 5). Notably, all the changes that occurred return to the initial value after a certain period of time due to the return of the variable that caused them to do so.

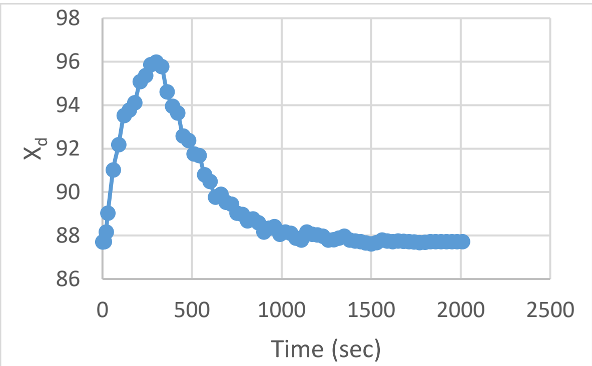

Fig. 2. Response of the light compound fraction in the top product (X_d) to 50% pulse in reflux flow rate (R).

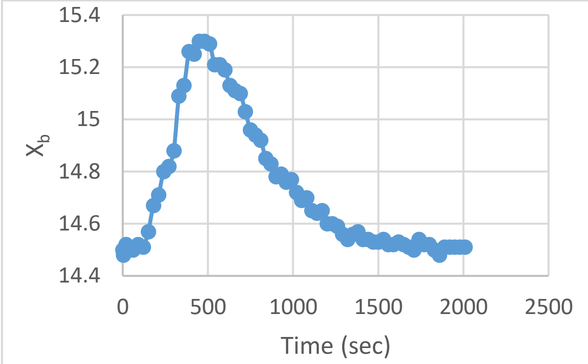

Fig. 3. Response of the light compound fraction in the bottom product (X_b) to 50% pulse in reflux flow rate (R).

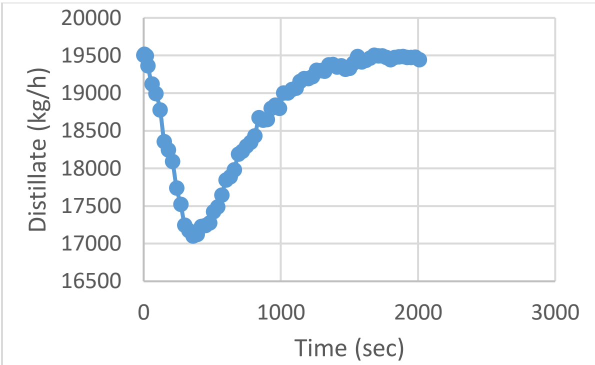

Fig. 4. Response of the distillate flow rate (D) to 50% pulse in reflux flow rate (R).

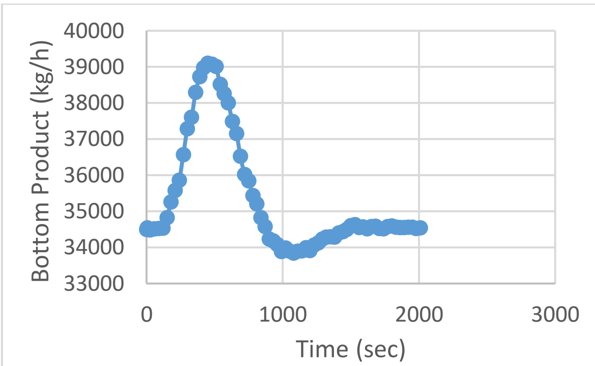

Fig. 5. Response of the bottom flow rate (B) to 50% pulse in reflux flow rate (R).

3.2 Pulse Heat Duty of Reboiler

When a pulse is applied to the heat input of the reboiler, the temperatures at the bottom and the top of the distillation column increase. These increases lead to a higher evaporation rate in the reboiler. Consequently, the distillate composition X_d decreases due to an increased presence of heavy components in the overhead product, while the total distillate flow rate D intensifies. In addition, the rise in bottom temperature reduces the fraction of light components in the bottom product. As a result, a decrease in X_b and in the bottom product flow rate is observed, as illustrated in Figs. 6, 7, 8 and 9. These trends are consistent with those reported in previous studies [7], [22], [24]. Once the reboiler heat input is restored to its initial value, all process variables gradually return to their original steady-state levels.

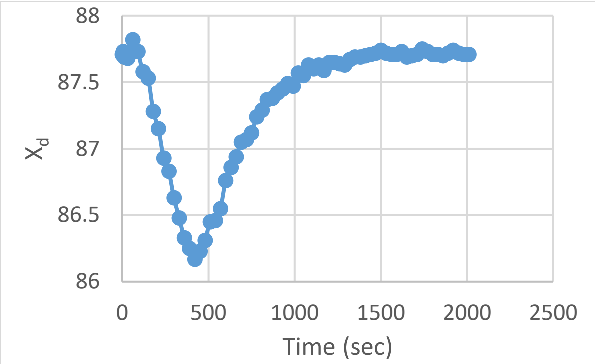

Fig. 6. Response of the light compound fraction in the top product (X_d) to 50% pulse in heat duty of reboiler.

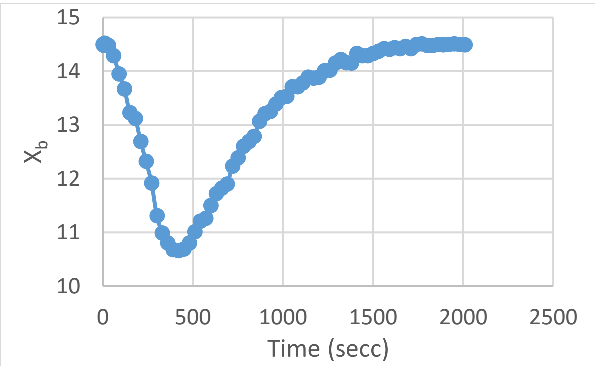

Fig. 7. Response of the light compound fraction in the bottom product (X_b) to 50% pulse in heat duty of reboiler.

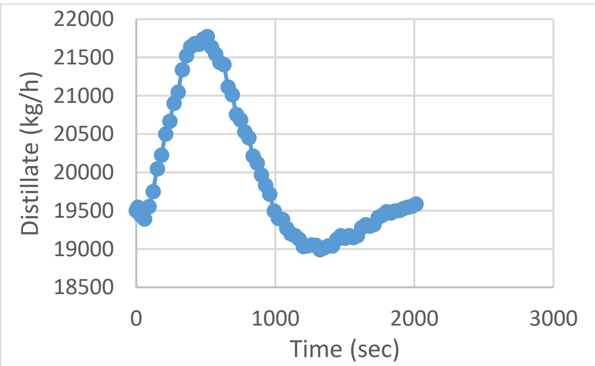

Fig. 8. Response of the distillate flow rate (D) to 50% pulse in heat duty of reboiler.

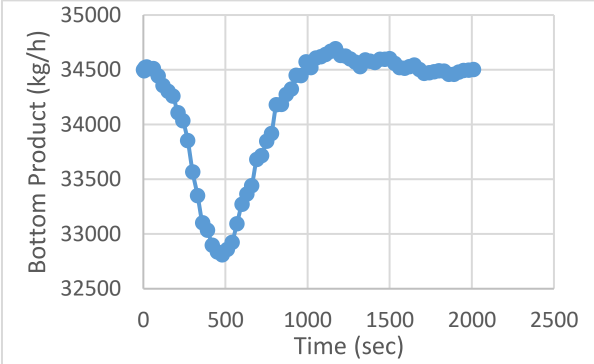

Fig. 9. Response of the bottom flow rate (B) to 50% pulse in heat duty of reboiler.

3.3 Pulse in Light Compound Fraction in the Feed (X_f)

The fraction of light components in the feed (X_f) was increased for 300 s, which resulted in higher vapour flow rates in the rectifying section and corresponding changes in the temperature and composition profiles. The increased presence of lighter components led to a reduction in column temperatures due to enhanced evaporation. With a constant reflux flow rate, the top-column temperature decreased, which reduced the concentration of heavy components and increased the fraction of light components in the distillate, as shown in Fig. 10. Consequently, the distillate flow rate increased (Fig. 12). In the stripping section, a slight decrease in temperature was observed, which increased the light component fraction in the bottom product (X_b) while reducing the bottom product flow rate, as illustrated in Figs. 11 and 13. These results are consistent with those reported in previous studies [7], [14], [25].

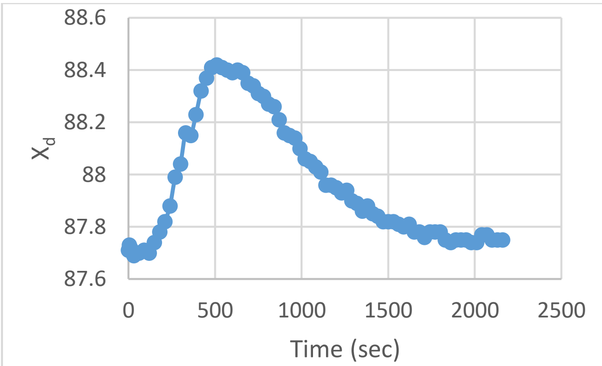

Fig. 10. Response of the light compound fraction in the top product (X_d) to 30% pulse in light compound fraction in the feed (X_f).

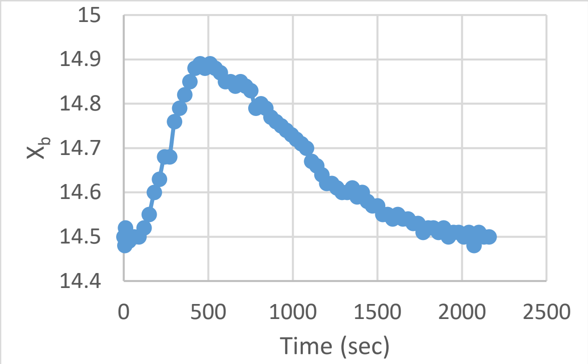

Fig. 11. Response of the light compound fraction in the bottom product (X_b) to 30% pulse in light compound fraction in the feed (X_f).

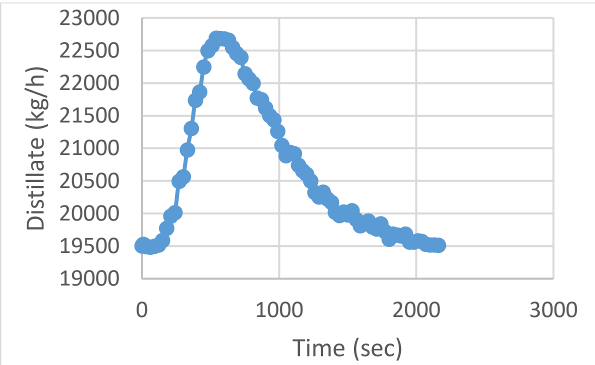

Fig. 12. Response of the distillate flow rate (D) to 30% pulse in light compound fraction in the feed (X_f).

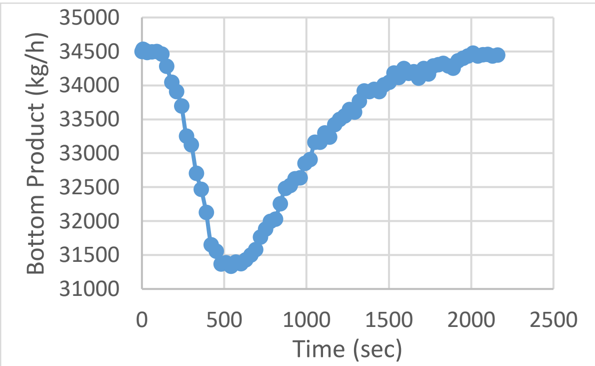

Fig. 13. Response of the bottom flow rate (B) to 30% pulse in light compound fraction in the feed (X_f).

3.4 Pulse in Distillation Column Feed (F)

A pulse increase of 31% in the distillation column feed results in noticeable increases in X_d, X_b, D and B, as shown in Figs. 14, 15, 16 and 17. With constant reboiler heat input and reflux flow rate, the increased feed rate leads to a decrease in the top and bottom column temperatures. These temperature reductions decrease the concentration of heavy components (C7+) in the upper section, which increases the fraction of light components in the distillate. Similarly, the lower temperature in the bottom section increases the fraction of light components retained in the bottom product. Moreover, the higher feed rate naturally results in increased flow rates of the distillate and the bottom product. These results are consistent with the findings reported in previous studies [7], [25].

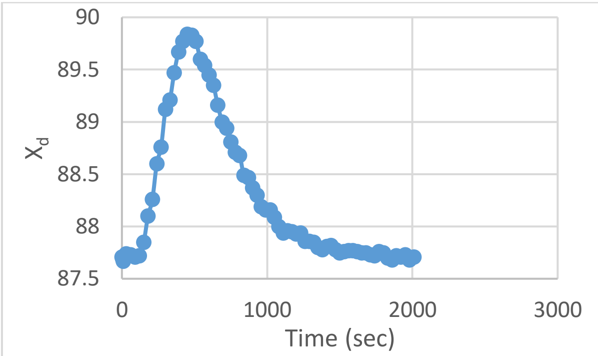

Fig. 14. Response of the light compound fraction in the top product (X_d) to 30% pulse in distillation column feed (F).

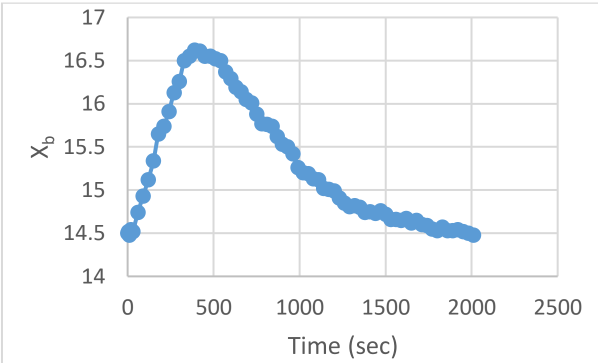

Fig. 15. Response of the light compound fraction in the bottom product (X_b) to 30% pulse in the distillation column feed (F).

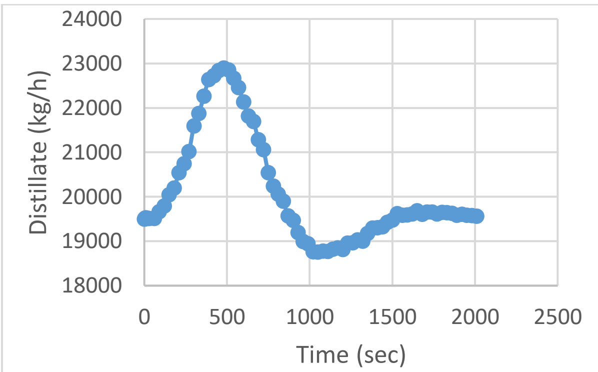

Fig. 16. Response of the distillate flow rate (D) to 30% pulse in the distillation column feed (F).

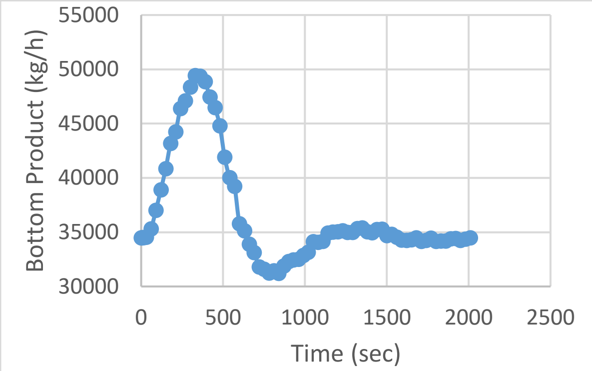

Fig. 17. Response of the bottom flow rate (B) to 30% pulse in the distillation column feed (F).

System identification is the process of using measurable input–output data to create mathematical models of dynamic systems. The procedure involves introducing known input signals into a system and documenting the output response result. The parameters of a model that best capture the dynamics of the system are then estimated using these data sets.

System identification is essential for designing accurate control systems, especially in complex applications such as chemical processes, robotics and biomedical systems where theoretical modelling is challenging. By providing reliable process models, the performance of controllers such as PID and MPC is improved, which effectively links mathematical models with real-world system behaviour.

Linear time-invariant systems benefit greatly from pulse response modelling, which offers insights into system characteristics such as stability, time delay, rising time and settling behaviour; thus, it is appropriate for assessing systems with intricate or unknown internal dynamics [5], [26]–[28].

The steady-state gain (k), time constant (τ) and time delay (τ_D) are calculated based on the time domain response. Firstly, a Bode diagram is drawn using MATLAB, based on the time-domain response of each response [29]. Then, the parameters are calculated from the Bode diagram as [30], [31].

For the first order, by plotting bode plot for the response of light compound fraction in the top product (X_d) for pulse in reflux flow rate and calculating the transfer function parameters from the plotting (Fig. 18),
For the first order, the slope of the high-frequency asymptote (HFA) must be equal (−20 dB/decade)

$$Log\ Modulus\ (dB) = 20 Log\ k \quad \ldots(18)$$

where k is the steady-state gain, which is the intersection between low-frequency asymptote (LFA) and y-axis on Bode plot.

$$w_c = \frac{1}{\tau} \quad \ldots(19)$$

where w_c is the critical frequency, which is the intersection between LFA and HFA on Bode plot.

$$\emptyset^o = -45 - \frac{\tau_D}{\tau}\left(\frac{180}{\pi}\right) \quad \ldots(20)$$

where $\emptyset^0$ is the phase angle (deg), which is the intersection between w_c and phase plot.

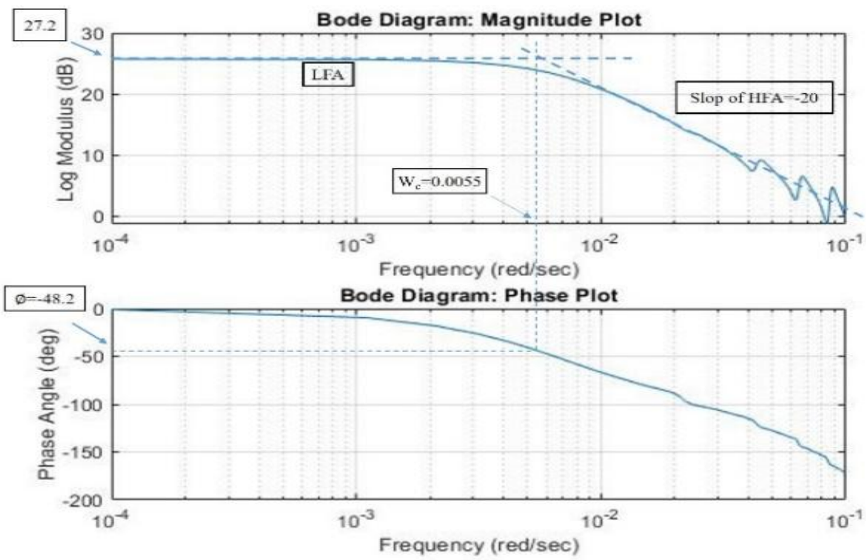

Fig. 18. Bode plot for the response of light compound fraction in the top product (X_d) for a pulse in reflux flow rate

Then,

$$G_{11} = \frac{23}{(182s+1)} e^{-10s} \quad ...(21)$$

For the second order, by plotting bode plot for the response of the light compound fraction in the bottom product (X_b) for pulse in reflux flow rate and calculating the transfer function parameters from the plotting (Fig. 19),

For the second order, the slope of the HFA (2) (HFA2) must be equal (−40 dB/decade)

$$Log\ Modulus\ (dB) = 20Log\ k \quad ...(22)$$

$$w_{c1} = \frac{1}{\tau 1} \quad ...(23)$$

where w_{c1} is the critical frequency (1), which is the intersection between LFA and HFA (1) (HFA1) on Bode plot.

$$w_{c2} = \frac{1}{\tau 2} \quad ...(24)$$

where w_{c2} is the critical frequency (2), which is the intersection between HFA1 and HFA2 on Bode plot.

$$\emptyset^o = -45 + \tan^{-1} - \frac{\tau_1}{\tau_2} - \frac{\tau_D}{\tau_2}\left(\frac{180}{\pi}\right) \quad ...(25)$$

where $\emptyset^0$ is the phase angle (deg), which is the intersection between w_{c2} and phase plot.

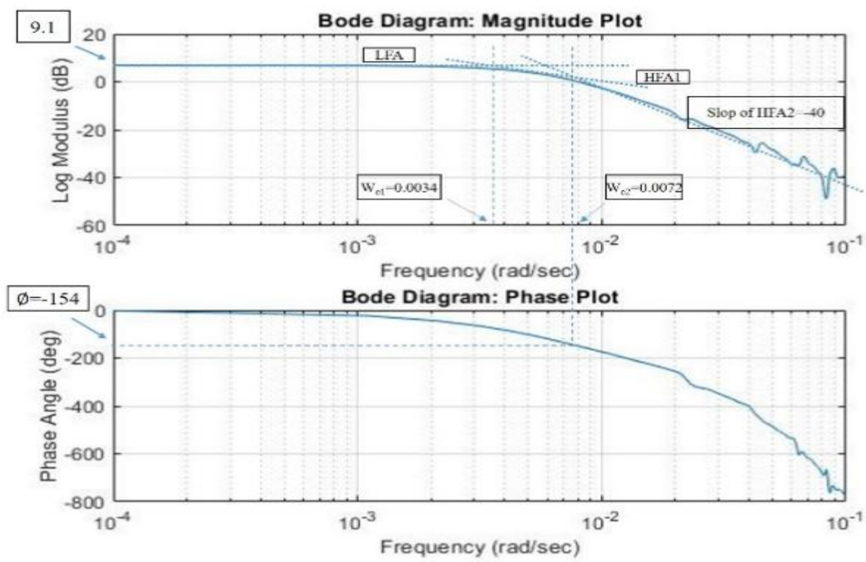

Fig. 19. Bode plot for the response of light compound fraction in the top product (X_d) for a pulse in reflux flow rate

Then,

$$G_{21} = \frac{2.85}{(139s+1)(294s+1)} e^{-108s} \quad ...(26)$$

Similarly, the other transfer functions obtain Equation (27). Model validation was performed by comparing the calculated model outputs with experimental data after applying same pulse, as presented in Figs. 20 and 21, where the results indicate an agreement exceeding 93%.

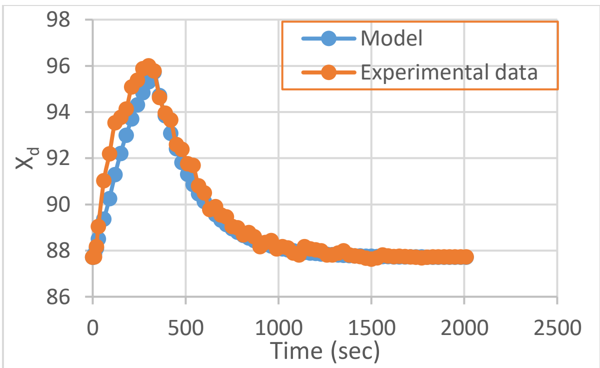

Fig. 20. Model and experimental data for G_{11}

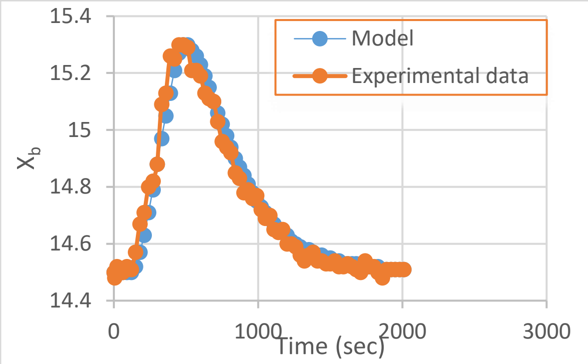

Fig. 21. Model and experimental data for G_{21}

$$\begin{bmatrix} X_D \\ X_B \\ D \\ B \end{bmatrix} = \begin{bmatrix} \frac{23e^{-10s}}{(182s+1)} & \frac{-0.52e^{-50s}}{(111s+1)(185s+1)} & \frac{14.13e^{-85s}}{(218s+1)(333s+1)} & \frac{0.53e^{-70s}}{(122s+1)(263s+1)} \\ \frac{2.85e^{-108s}}{(139s+1)(294s+1)} & \frac{-1.68e^{-39s}}{(150s+1)(250s+1)} & \frac{8.9e^{-101s}}{(278s+1)(357s+1)} & \frac{0.56e^{-42s}}{(137s+1)(313s+1)} \\ \frac{-2.82e^{-24s}}{(175s+1)(303s+1)} & \frac{0.18e^{-63s}}{(210s+1)(270s+1)} & \frac{13e^{-113s}}{(210s+1)(244s+1)} & \frac{0.24e^{-65s}}{(132s+1)(192s+1)} \\ \frac{3.1e^{-120s}}{(147s+1)(175s+1)} & \frac{-0.135e^{-72s}}{(154s+1)(192s+1)} & \frac{-14.2e^{-90s}}{(208s+1)(320s+1)} & \frac{0.9e^{-28s}}{(110s+1)(139s+1)} \end{bmatrix} \begin{bmatrix} R \\ Q_R \\ X_f \\ F \end{bmatrix} \quad \ldots(27)$$

4. Conclusion

In this study, a dynamic empirical model for a multicomponent distillation column with MIMO is developed using the LV configuration. Equation (27) represents the empirical model and is expressed as a 4×4 matrix comprising 16 transfer functions (most of them are second order), each describing the dynamic relationship between a manipulated variable and a corresponding controlled variable. This modelling approach not only helps understand the inherent complexity of distillation column dynamics but also lays the groundwork for developing advanced control strategies, such as FLC, MPC or others, to enhance process stability and efficiency.

Notation

B Bottom product flow rate (kg/h)
C Heat capacity (Kj/kg °C)
D Distillate product flow rate (kg/h)
F Feed flow rate (kg/h)
H_f Feed enthalpy (Kj/h)
H^l Enthalpy of liquid phase (Kj/h)
H^v Enthalpy of vapour phase (Kj/h)
L Liquid flow rate (kg/h)
M Liquid holdup (kg)
N Total number of trays
Q_c Heat amount reduced by condenser (Kj/h)
P Pressure (kg/cm^2)
Q_R Heat amount supply by reboiler (Kj/h)
R Reflux flow rate (kg/r)
T Temperature (°C)
V Vapour flow rate (kg/h)
x Liquid concentration
x_f Feed concentration
y Vapour concentration
τ Time constant in (sec)
τ_D Time delay in (sec)
α Relative volatility
γ Correction factor for liquid ideality
φ Correction factor for vapour ideality

Subscription

1 Tray number one
b Bottom of the column
d Overhead reflex drum
i For any component
n For any tray except feed tray
nf Feed tray
R Reflux

Superscription

T Total
* Saturation state

Conflicts of Interest

The authors declare no conflicts of interest regarding the publication of this paper.

References

[1] A. A. de Morais Júnior, J. C. Finiz Filho, L. O. A. Rojas, and R. P. Brito, “Inferential control strategies using neural soft sensor in a high purity distillation column,” Caderno Pedagógico, vol. 21, no. 5, pp. e4402–e4402, 2024.

[2] V. K. P.Domingos, N. Manuel, C. M. M. Faria, F. R. Cangue and A. A. Ch. Barros “Numerical simulation of oil refining tower” Studies in Engineering and Exact Sciences, Curitiba, v.5, n.2, p. 01-27, 2024

[3] A. Wahid, “Distillation Column Control using Multiple Model Predictive Control based on Representative Model Predictive Control Method,” no. October, 2015.

[4] W. L. Luyben, *Process Modeling, Simulation, and Control for Chemical Engineers*, 2nd ed. New York, NY, USA: McGraw-Hill, 1996.

[5] R. Rengaswamy, B. Srinivasan, and N. P. Bhatt, Process Control Fundamentals. New Delhi, India: Springer India, 2020.

[6] B. Mahmoudzadeh and M. Masoumi, “Dynamic simulation and control of a distillation column using Effective Relative Gain Array,” World Academy of Science, Engineering and Technology, vol. 76, Apr. 2011.

[7] C. Fuentes and W. L. Luyben, “Control of High-Purity Distillation Columns,” 1983. doi: 10.1021/i200022a004.

[8] A. Al-Jlibawi, M. L. Bin Othman, M. S. Al-Huseiny, I. Bin Aris, and S. Bahari, “The efficiency of soft sensors modelling in advanced control systems in oil refinery through the application of hybrid intelligent data mining techniques,” Journal of Physics: Conference Series, vol. 1529, no. 5, pp. 0–12, 2020, doi: 10.1088/1742-6596/1529/5/052049.

[9] V. D. Hajare and B. M. Patre, “Decentralized PID controller for TITO systems using characteristic ratio assignment with an experimental application,” ISA Transactions, vol. 59, pp. 385–397, 2015, doi: 10.1016/j.isatra.2015.10.008.

[10] C. Pătruţ, C. S. Bîldea, I. Liţă, and A. A. Kiss, “Cyclic distillation - Design, control and applications,” Separation and Purification Technology, vol. 125, pp. 326–336, 2014, doi: 10.1016/j.seppur.2014.02.006.

[11] A. Wahid and Z. H. Brillianto, “Multivariable model predictive control (4x4) of methanol-water separation in dimethyl ether production,” AIP Conference Proceedings, vol. 2255, no. September, 2020, doi: 10.1063/5.0013764.

[12] E. R. Baliyan and Akram Taher Ahmed Ali Al Zubidai, “A Studt on Mathmatical Modelling of Distillation Column in A Petroleum Process" IJARIIE-ISSN(O)-2395-4396, Vol-6, Issue-2, 2020.

[13] L. Tugashova, R. Bazhenov, U. Abdyldaeva, I. Korosteleva, and E. Muromtseva, “A simulation modeling approach used in the crude oil refining process,” in Journal of Physics: Conference Series, IOP Publishing, 2022, p. 62003.

[14] H. S. Truong, I. Ismail, and R. Razali, “Fundamental Modeling and Simulation of a Binary Continuous Distillation Column,” 2010.

[15] Z. Abdullah, N. Aziz, and Z. Ahmad, “Nonlinear modelling application in distillation column,” Chemical Product and Process Modeling, vol. 2, no. 3, 2007.

[16] A. Panadourakis, M. F. Doherty, and J. M. Douglas, “Approximate Dynamic Models for Chemical Process Systems,” 1989. doi: 10.1021/ie00089a008.

[17] B. Wittgens and S. Skogestad, “Evaluation of dynamic models of distillation columns with emphasis on the initial response,” 2000. doi: 10.4173/mic.2000.2.2.

[18] A. Maro, Naufal Wahid and Syafiq, “Multi Input Multi Output (MIMO) Control 2x2 at Vacuum Distillation Unit for LVGO, MVGO, and HVGO Production,” E3S Web of Conferences, vol. 67, pp. 1–5, 2018, doi: 10.1051/e3sconf/20186703012.

[19] A. Wahid and R. Adi, “Modeling and Control of Multivariable Distillation Column Using Model Predictive Control Using Unisim,” Sinergi, vol. 20, no. 1, p. 14, 2016, doi: 10.22441/sinergi.2016.1.003.

[20] J. Drgoňa, M. Klaučo, R. Valo, J. Bendžala, and M. Fikar, “Model identification and predictive control of a laboratory binary distillation column,” Proceedings of the 2015 20th International Conference on Process Control, PC 2015, vol. 2015-July, pp. 357–362, 2015, doi: 10.1109/PC.2015.7169989.

[21] W. L. Luyben, Distillation Design and Control Using Aspen Simulation, Hoboken, NJ, USA: John Wiley & Sons, 2013.

[22] S. Skogestad, “Dynamics and control of distillation columns A tutorial introduction,” *Chemical Engineering Research and Design*, vol. 75, no. 6, pp. 539–562, 1997.

[23] G. H. Miller, “Distillation Theory,” Whisky Science, pp. 295–376, 2024, doi: 10.1007/978-3-031-50687-1_7.

[24] P. A. Martin, D. Odloak, and F. Kassab,

"Robust model predictive control of a pilot plant distillation column," Control Engineering Practice, vol. 21, no. 3, pp. 231–241, 2013, doi: 10.1016/j.conengprac.2012.10.004.

[25] S. Skogestad and M. Morari, "The dominant time constant for distillation columns," 1987. doi: 10.1016/0098-1354(87)87006-0.

[26] L. Chen, J. Li, and R. Ding, "Identification for the second-order systems based on the step response," 2011. doi: 10.1016/j.mcm.2010.11.070.

[27] N. S. Nise, "Control System Engineering," 8th edition. Hoboken, NJ, USA: John Wiley &Sons, 2019.

[28] L.Stocco, "Optimal 2nd Order LTI System Identification", in Proceedings of the 2023 IEEE/ASME International Conference on Advanced Intelligent Mechatronics (AIM), Seattle, WA, 28 June–1 July. IEEE, pp. 940–945, 2023. doi:10.1109/AIM46323.2023.10195736.

[29] M. L. Luyben and W. L. Luyben, "Essentials of Process Control McGraw-Hill Chemical Engineering Series," Essentials of Process Control, p. 584, 1997.

[30] D. Tebaldi and R. Zanasi, "The Construction of Asymptotic Bode Plots: A New Direct Method," 2025, [Online]. Available: http://arxiv.org/abs/2503.21667

[31] A. K. Al-Dulaimi and Y. S. Al-Sabbar, Fundamentals of process control in Chemical Engineering, First Edit, unpublished manuscript, 2021.

نمذجة عمود تقطير متعدد المتغيرات (٤×٤) باستخدام التعرف على الأنظمة المعتمد على دالة النبضة

ليث صادق محمود[1*]، خالد مخلف موسى الزوبعي[2]
[1] شركة مصافي الوسط، وزارة النفط، بغداد، العراق*
[2] قسم الهندسة الكيمياوية، جامعة النهرين، بغداد، العراق
*البريد الالكتروني: layth.phche23@ced.nahrainuniv.edu.iq

المستخلص

تُعدّ أعمدة التقطير من أهم الوحدات في الصناعات الكيميائية والبتروكيميائية، وخاصةً في مصافي النفط. تهدف هذه الدراسة إلى إنشاء وتقييم نموذج تجريبي لعمود تقطير متعدد المكونات. وقد تم بناء نموذج تجريبي لتمثيل السلوك غير الخطي للعمود، حيث يُعامل كنظام ديناميكي متعدد المدخلات والمخرجات. يبلغ قطر أعمدة التقطير الصناعية المستخدمة في هذه الدراسة ٢,٢ متر، وارتفاعها ١٦,٦ متر، وهي مزودة بـ ٢٠ صينية صمامات. وتُشغّل هذه العملية حاليًا في مصفاة الدورة التابعة لشركة ميدلاند للتكرير في شرق بغداد، العراق. ولإيجاد النموذج الذي يصف النظام، تم اختيار أربعة متغيرات مُتحكَّم بها (معدل تدفق الارتداد، وحمل التسخين في المُسخِّن، ونسبة المكون الخفيف في التغذية، ومعدل تدفق التغذية) وأربعة متغيرات مُتحكَّم بها في المخرجات (نسبة المكون الخفيف في المنتج العلوي، ونسبة المكون الخفيف في المنتج السفلي، ومعدل تدفق المنتج العلوي، ومعدل تدفق المنتج السفلي). أُجريت التجارب بتطبيق نبضة لمدة ٣٠٠ ثانية على كل متغير من المتغيرات المُتحكَّم بها، مع تثبيت المتغيرات الأخرى. وقد تم الحصول على مصفوفة ٤×٤ تتكون من ١٦ دالة نقل (معظمها من الدرجة الثانية). تمثل كلّ معادلة العلاقة بين المتغيرات المُتحكَّم بها والمتغيرات الخاضعة للتحكم. تُشكل هذه المعادلات أساسًا لاستراتيجيات تحكم متقدمة، مثل التحكم المنطقي الضبابي، والتحكم التنبؤي بالنموذج، وغيرها من أساليب التحكم الحديثة.